Bonding and diffusion of Ba on a Si(001) reconstructed surface

Jun Wang, J. A. Hallmark, D. S. Marshall, and W. J. Ooms
Phoenix Corporate Research Labs, 2100 East Elliot Road, Tempe, Arizona 85284

Pablo Ordejón and Javier Junquera
Departamento de Física, Universidad de Oviedo, 33007 Oviedo, Spain

Daniel Sánchez-Portal, Emilio Artacho, and José M. Soler
Departamento de Física de Materia Condensada C-III, Universidad Autónoma de Madrid, 28049 Madrid, Spain
(Received 20 October 1998)

Bonding and diffusion of a Ba adatom on a Si(001) surface have been studied using first-principles density-functional calculations. It is found that the favorable bonding site of the adatom is the fourfold site located in the trough between Si dimer rows. The bonding between Ba adatom and the surface is shown to be only slightly ionic in character, with a small charge transfer from Ba to the substrate, and with an important covalent component. The calculated jumping rates show a strongly anisotropic diffusivity of Ba on the surface. [S0163-1829(99)00423-3]

Thin-film metal silicides have received great attention in recent years, due to their potential applications to very large-scale integration electronic circuits. The importance of alkaline-earth-metal silicides is boosting due to the demonstration that they are an essential step in the recently reported commensurate growth of crystalline oxides on a Si(001) surface.[1] These may essentially eliminate the fundamental limitations of the silica-based metal-oxide-semiconductor transistor technology, by providing better dielectric properties and cleaner, defect-free interfaces with silicon. The growth of the commensurate oxide was shown to depend critically on the formation of a submonolayer of alkaline-earth-metal silicide, which makes the interface with the oxide thermodynamically stable.

The properties of ultrathin barium silicide films grown on Si(001) have been measured using several techniques.[1-8] Low-energy electron diffraction[6] (LEED) and reflection high-energy electron diffraction[1,7] (RHEED) experiments show that submonolayers of Ba form ordered structures on Si(001). Model structures of the metal covered surface consistent with the obtained experimental results have been proposed. However, little is known about the detailed atomic arrangements and the driving forces of forming such ordered surface structures. Besides, there are important discrepancies in the experimental results, which can be clarified by means of first-principles calculations. For instance, some experiments seem to indicate an ionic interaction originated from a charge transfer from Ba to the Si surface. However, recent data[3] apparently contradict this observation, reporting no charge transfer for low coverage, absorbed states, while at higher coverage a silicide forms, which does show a significant charge transfer.

In this paper, we address the first stages of the deposition of Ba on Si(001), by means of *ab initio* quantum-mechanics calculations based in density-functional theory.[9] In particular, we study the interaction between a Ba adatom and a reconstructed Si(001) surface at very low coverage. We analyze the preferential absorption sites, and the nature of bonding. We also focus on the kinetic properties of the adatom on the surface. An estimate is given for the predicted epitaxial growth temperature of Ba on Si(001) using simplified transient state theory, and a growth model is proposed from our results.

The SIESTA program,[10] used in this paper to calculate the energies and atomic forces, is a self-consistent density-functional approach that utilizes the local-density approximations on exchange and correlation potential[11] and separable[12] normconserving Troullier-Martins[13] pseudopotentials. Pseudoatomic orbitals of Sankey-Niklewski type,[14] generalized to include multiple-ζ and polarization functions[15] are used to represent the valence wave functions. We found it necessary to include the Ba semicore $5p$ shell in the valence to achieve reliable results. The inclusion of the empty $5d$ shell also affects the results significantly, and therefore, these shells are included in the atomic orbitals basis set.

The global and metastable bonding sites of the adatom on the surface are determined using an energy-mapping scheme.[16] For a given (x,y) position of the Ba atom on the surface, the system is relaxed to find the energy minimum [maintaining the fixed (x,y) coordinates of the adatom, and relaxing both its vertical position and the coordinates of the substrate Si atoms]. The results are shown in Fig. 1. The irreducible surface area, indicated by the dotted lines in Fig. 1, is evenly covered by a mesh of (5×9) points where the potential energy of a Ba adatom is sampled. A slab geometry is used in our simulations. The supercell consists of 4 atomic layers of Si, with 16 Si atoms per atomic layer. The dangling bonds of the bottom Si atoms (which are kept fixed at their bulk lattice position) are tied up using hydrogen atoms. This hydrogen saturation allows us to use a slab much thinner than the one that would be required if the calculations were done with two equivalent surfaces. It was checked that further increasing the slab thickness does not change the simulation results significantly. For instance, the difference in energy between the *A* and *B* bonding sites (see below) changed

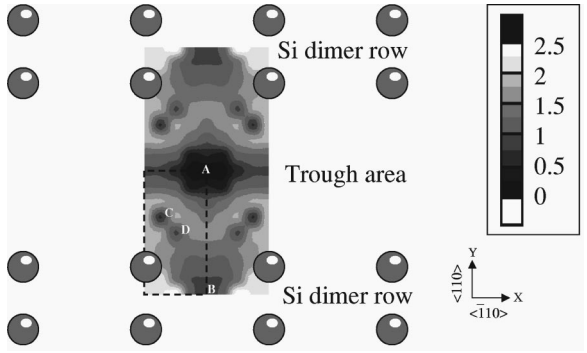

FIG. 1. Surface potential energy map (in eV) of a Ba atom on a Si(001). A sketch of the dimer rows in the (2×1) reconstruction is shown as a reference to the energy map.

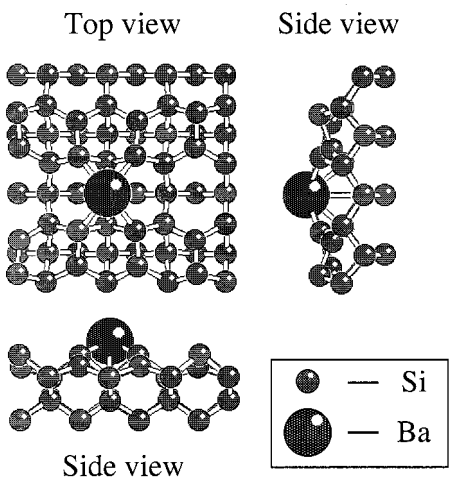

FIG. 2. Minimum energy structure of a Ba adatom on the Si(001) surface.

only about 0.05 eV (which amounts to a mere 6%), when a slab with six atomic layers instead of four was used.

For the clean Si(001) surface, our method correctly predicts the $c(4\times2)$ reconstruction to be the most stable. For the real dynamics of the adatoms at moderately high temperatures the pattern of dimer buckling is not expected to be important, due to the small energy difference between different patterns in comparison with the thermal and Ba-Si bond energies. In the calculation of the energy map, however, the results can be sensitive to the initial pattern, since different local minima can be found starting from different configurations. The results shown in Fig. 1 correspond to the lowest energy minimum found starting with different patterns of the initial dimer buckling.

From the potential energy map we identify the most favorable bonding site of the adatom to be at the fourfold site between the dimer rows, denoted as *A* in Fig. 1. These sites are surrounded by 4 dimers with the up atoms pointing towards the absorbed Ba, and their energy is 0.8 eV lower than any of the other potential wells identified on the surface. The final atomic structure of Ba at this bonding site is given in Fig. 2. It can be seen that a Ba atom does not break any of the four Si dimers to which it is bonded. However, they are pulled toward the Ba atom to satisfy the optimum bondlength between Ba and Si on surface. As a result of the interaction, two consecutive Si dimers in the row are buckled in the same direction toward the Ba adatom, which leads to a solitonlike defect in the original $c(4\times2)$ pattern. If we force the dimer buckling to follow the $c(4\times2)$ pattern and redo the calculation, we end up with a metastable structure that has an energy of about 0.6 eV higher than that shown in Fig. 2. This energy difference is much larger than the energy necessary to reverse the buckling direction of a dimer in the clean reconstructed Si(001) surface. We then expect that the presence of adsorbed Ba atoms will determine the pattern of buckling, at least for low coverage. Recent scanning tunneling microscopy (STM) experiments[8] have also identified the fourfold site between dimer rows as the most common absorption site of Ba on Si(001). Our results confirm the interpretation of these experiments. It is also clear in the STM images that the presence of the Ba atom in this site stabilizes the buckling of the dimer in its vicinity.

The bond-length between Ba and Si on the surface is 3.25 ± 0.005 Å and there are six such bonds formed when Ba is at site *A*. Four of the six bonds are formed laterally with the first-layer Si atoms. The other two are backbonds with the second-layer Si atoms. One additional backbond is formed between Ba and a third-layer Si atom with a bondlength of 3.78 Å , slightly stretched from the ideal case. The formation of the backbonds pulls the Ba adatom deeply into the trough area between Si dimer rows. The height difference between the Ba and the surrounding Si atoms is only 0.96 Å, which is comparable with the height difference of the two Si atoms in a buckled Si dimer. The structure of the dimers which are bonded to the adatom is essentially the same as that of the dimers in the clean surface.

Ba has an electronegativity of 0.89, which is much smaller than that of Si, 1.90.[16] One would, therefore, expect some charge transfer to occur when Ba interacts with Si on the surface. However, Mulliken population analysis shows that the charge transferred from the adatom to the surface is of only about 0.15 *e*. There is, nevertheless, a large redistribution of the charge in the surroundings of the Ba. This can be also inferred from the Mulliken charges, which show that the $6s$ orbital of Ba has only 0.45 electrons, while the remaining 1.4 electrons of the adatom are located in the $6p$ and $5d$ orbitals. This suggests the formation of a covalent bonding between the adatom and the surface. We have further analyzed the character of the bonding by plotting the redistribution of the charge density. This is obtained by subtracting, from the system charge density, a reference constructed by adding the densities of an isolated Ba atom and the free substrate (with positions fixed at the final-relaxed location shown in Fig. 2). This three-dimensional (3D) charge density $Q(x,y,z)$ is projected onto the $x-y$ plane: $q(x,y)=\int_{-\infty}^{\infty}Q(x,y,z)dz$, and shown in Fig. 3. The negative and positive differentials of the projected charge density are shown separately in Figs. 3(a) and 3(b), respectively. The integrated intensity in either figure gives the total amount of the charge that is redistributed upon the formation of the bond, which amounts to 0.58 *e*. This value is much larger than the charge transfer obtained by the Mulliken analysis, indicating that the bonding is mainly covalent. The areas where the charge is removed are localized around the Ba adatom. This charge is redistributed to the surface atoms. There is a significant buildup of charge in the zone between the dangling bond of the up atom in the dimers and the Ba

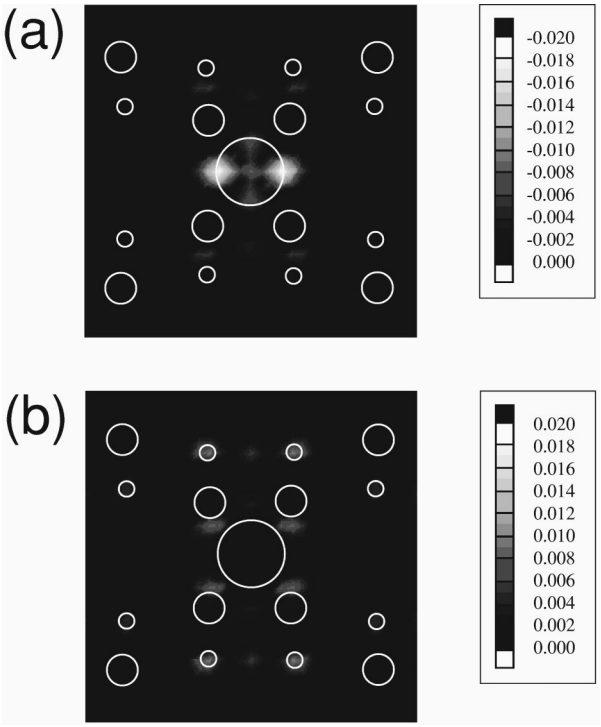

FIG. 3. Gray scale image showing the negative (a) and positive (b) differentials of the charge density of a Ba adatom at its global bonding site with respect to the reference charge density. The unit is in electron charges. White circles in the figure indicate the positions of the Ba adatom, the largest circle, and the first-layer Si atoms. The size of the circle reflects the height of the Si atom with larger circles being closer to the viewer.

atoms. This indicates again the formation of a directional, covalent bonding between the adatom and the surface. There is also a significant redistribution of charge in the down atoms in the dimer (mainly from the covalent bond within the dimer to the down atom dangling bond). As indicated by Mulliken population analysis, the net charge of the Si dimer atoms does not significantly change upon Ba adsorption, although there is certainly some charge transfer from the Ba region to zones quite distant.

From the above charge analysis, we conclude that the bonding of the Ba adatom to the substrate has a strong covalent character, with a slight charge transfer from the Ba atom. This confirms and explains the core-level shift experimental results of Cheng *et al.*,[3] who find a small or zero charge transfer at low coverage, in contrast with the ionic character of the metal silicides obtained at higher coverage (above 1 monolayer). This result is also consistent with the STM experiments,[8] which indicate only a partial charge transfer from Ba to the surface, as shown in our calculations.

Another noticeable metastable bonding site of Ba on the Si(001) surface is the fourfold site on top of a dimer row, denoted by *B* in Fig. 1. The energy of Ba at site *B* is 0.88 eV higher than it is at site *A* and the number of bonds it forms with the Si surface is also six, only two of which are at the optimum bond length, i.e., 3.25 Å. The height of Ba at site *B* is 0.71 Å higher than it is at site *A*. The presence of the Ba atom at site *B* does not introduce significant disturbance to the surrounding Si dimer rows. There are two additional metastable bonding sites indicated by letters *C* and *D* in Fig. 1. These bonding sites are not expected to play a significant role in Ba growth on Si(001) surface due to their relative weaker bonding strength and smaller collection area in comparison with that of *A* and *B*.

We now address the diffusivity of the Ba adatom on the surface, and estimate the epi-growth temperature of Ba on Si(001) surface. Using the potential energy map of Fig. 1, the diffusion pathway of Ba on Si(001) can be identified. The escaping rates of the Ba adatom from its global bonding site are estimated along two orthogonal directions, namely $\langle \bar{1}10 \rangle$ and $\langle 110 \rangle$, on the Si(001) surface (see Fig. 1). These rates are directly related to the diffusivity of Ba on the Si(001) surface at low-Ba coverage. From transient state theory, the rate at which an atom makes a specific jump follows the simple Boltzmann relationship

$$\Gamma_\alpha = \nu_\alpha \exp(-\Delta G_\alpha / k_B T), \tag{1}$$

where ν_α is the attempting rate of the atom in making such a jump, k_B is the Boltzmann constant, and ΔG_α is the activation-free energy. The ratio between the jumping rate along $\langle \bar{1}10 \rangle$ and $\langle 110 \rangle$ is then

$$\frac{\Gamma_{\langle \bar{1}10 \rangle}}{\Gamma_{\langle 110 \rangle}} = \frac{\nu_{\langle \bar{1}10 \rangle}}{\nu_{\langle 110 \rangle}} \exp[(\Delta S_{\langle \bar{1}10 \rangle} - \Delta S_{\langle 110 \rangle})/k_B] \times \exp[(\Delta E_{\langle 110 \rangle} - \Delta E_{\langle \bar{1}10 \rangle})/k_B T], \tag{2}$$

where ΔS_α and ΔE_α are the activation entropy and energy, respectively. Since we are interested only in an estimate of the jumping ratio, we will follow an often standard practice and assume that the entropy has a weak-directional dependence, i.e., $\Delta S_{\langle \bar{1}10 \rangle} \approx \Delta S_{\langle 110 \rangle}$. Also, we will replace the attempting rate of an atom by an estimate of its vibrational frequency at zero temperature, i.e., $\nu_\alpha \approx (1/2\pi)\sqrt{k_\alpha / m}$, where k_α is a spring constant in the direction of diffusion and m is the mass of the atom. Since the attempting rates enter only in the prefactor of the exponentials, the errors associated with this severe approximation will not be relevant for the estimate of the order of magnitude of the escaping ratio. The spring constants ν_α are obtained by fitting the total energies of the Ba atom as a function of its displacement from site *A* along $\langle \bar{1}10 \rangle$ and $\langle 110 \rangle$ to a quadratic function. The activation energy is determined by the smallest energy barrier to accomplish the jump along the given direction. The calculated values of the spring constants and the activation energies are 0.92 eV/Å and 0.95 eV, respectively, for the $\langle \bar{1}10 \rangle$ direction, and 1.20 eV/Å and 1.39 eV, respectively, for the $\langle 100 \rangle$ direction. With these values, the escaping ratio of Eq. (2) is estimated as to be about 2×10^7 at room temperature. In other words, the number of successful jumps is 2×10^7 times larger for the $\langle 110 \rangle$ than for the $\langle 110 \rangle$ direction. This indicates a highly anisotropic diffusion behavior, the preferred direction of diffusion being the trough between Si dimer rows.

The fact that both the preferential direction of diffusion and the bonding site are along the trough area between Si dimer rows suggests a one-dimensional growth behavior of Ba on Si(001). The trough area serves as a strong sink to the Ba adatoms, which after being trapped in the trough, can still move along it relatively easily to find its optimum growth site. This will lead to the formation of Ba chains located

between the Si rows. The epigrowth temperature of forming such chains can be estimated with respect to the Si homoepigrowth temperature using the following equation,

$$\left(\frac{k^{Si}}{m^{Si}}\right)^{1/2} e^{-\Delta E^{Si}/k_B T^{Si}} \approx \left(\frac{k^{Ba}}{m^{Ba}}\right)^{1/2} e^{-\Delta E^{Ba}/k_B T^{Ba}}, \qquad (3)$$

where T^{Si}, ΔE^{Si}, k^{Si}, and m^{Si} are epigrowth temperature, activation energy, spring constant, and mass for Si, respectively, and T^{Ba}, ΔE^{Ba}, k^{Ba}, and m^{Ba} are the corresponding quantities for Ba. Using the reported values for the Si epigrowth temperature[17] and the activation energy[16] of Si on Si(001) (750 K and 0.8 eV, respectively), the epigrowth temperature of Ba on Si(001) is estimated to be about 910 ± 10 K [using $(k^{Si}m^{Si})/k^{Ba}m^{Ba} \approx 4 \pm 1$]. Further study is under way to determine the structures of the Ba chains on Si(001).

In conclusion, we have reported the results of *ab initio* calculations of Ba absorption and diffusion on a Si(001) surface. The preferred bonding site is the fourfold site between Si dimer rows and the bonds made between Ba and the surface are only weakly ionic in character. The diffusivity is highly anisotropic, what is expected to cause an anisotropic growth of Ba on Si(001). Ordered structures, consisting of Ba atoms located in the trough areas between Si dimer rows, are expected to form at about 910 K, a temperature about 160 K higher than that of Si homoepigrowth.

We acknowledge partial support by Spain's DGES Grant No. PB-0202. P.O. acknowledges financial support from Motorola PCRL.

[1] R. A. McKee, F.J. Walker, and M. F. Chisholm Phys. Rev. Lett. **81**, 3014 (1998).

[2] R. T. Tung, J. M. Poate, J. C. Bean, J. M. Gibson, and D. C. Jacobson, Thin Solid Films **93**, 77 (1982); Raymond T. Tung, in *Silicon-Molecular Beam Epitaxy*, edited by Erich Kasper and John C. Bean (CRC Press, Boca Raton, 1988), Vol. II, p. 13.

[3] Chiu-Ping Cheng, Ie-Hong Hong, and Tun-Wen Pi, Phys. Rev. B **58**, 4066 (1998), and references therein.

[4] K. Ojima, S. Hongo, and T. Urano, Surf. Sci. **402-404**, 150 (1998).

[5] Y. Takeda, T. Ohtani, K. Ojima, T. Urano, and S. Hongo, J. Electron. Spectrosc. Relat. Phenom. **88-91**, 619 (1998); Y. Takeda, T. Urano, T. Ohtani, K. Tamiya, and S. Hongo, Surf. Sci. **402-404**, 692 (1998).

[6] W. C. Fan, N. J. Wu, and A. Ignatiev, Phys. Rev. B **42**, 1254 (1990); W. C. Fan and A. Ignatiev, Surf. Sci. **253**, 297 (1991).

[7] R. A. McKee, F. J. Walker, J. R. Conner, and R. Raj, Appl. Phys. Lett. **63**, 2818 (1993).

[8] X. Yao, X. Hu, D. Sarid, Z. Yu, J. Wang, D. S. Marshall, R. Droopad, J. K. Abrokwah, J. A. Hallmark, and W. J. Ooms, Phys. Rev. B **59,** 5115 (199).

[9] W. Kohn and L. Sham, Phys. Rev. **140**, 1133 (1965).

[10] P. Ordejón, E. Artacho, and J. M. Soler, Phys. Rev. B **53**, 10 441 (1996); D. Sánchez-Portal, P. Ordejón, E. Artacho, and J. M. Soler, Int. J. Quantum Chem. **65**, 453 (1997).

[11] D. M. Ceperley and B. J. Alder, Phys. Rev. Lett. **45**, 566 (1980); J. P. Perdew and A. Zunger, Phys. Rev. B **23**, 5048 (1981).

[12] L. Kleinman and D. M. Bylander, Phys. Rev. Lett. **48**, 1425 (1982).

[13] N. Troullier and J. L. Martins, Phys. Rev. B **43**, 1993 (1991).

[14] O. F. Sankey and D. J. Niklewski, Phys. Rev. B **40**, 3979 (1989).

[15] D. Sánchez-Portal, P. Ordejón, E. Artacho, and J. M. Soler (unpublished).

[16] Jun Wang and A. Rockett, Phys. Rev. B **43**, 12 571 (1991); Jun Wang, D. A. Drabold, and A. Rockett, Appl. Phys. Lett. **66**, 1954 (1995).

[17] R. J. Hamers, U. K. Khler, and J. E. Demuth, J. Vac. Sci. Technol. A **8**, 195 (1990).